Dynamic Characteristics of S-Band DC SQUID Amplifier

Georgy V. Prokopenko, Sergey V. Shitov, Irina L. Lapitskaya, Valery P. Koshelets, and Jesper Mygind

***Abstract*—A low-noise rf amplifier based on a dc SQUID (SQA) has been tested in the frequency range 3.0–4.6 GHz in the open-loop configuration. The following parameters have been measured for the single-stage balanced type SQA at 4.0 GHz: gain (12 ± 1) dB, 3 dB bandwidth of 500 MHz and noise temperature (1.0 ± 0.25) K. For the nonbalanced type SQA at 4.0 GHz gain was (15 ± 1) dB, 3 dB bandwidth 200 MHz and noise temperature (0.5 ± 0.25) K. The improved performance is obtained due to the increased characteristic voltage (≈ 420 μV) of the small-area (down to 0.7–0.9 μm^2) high-quality Nb-AlO$_x$-Nb SIS junctions. The saturation power (normalized to 1 GHz) referred to the input at 1 dB gain compression is estimated as ≈ 55 K*GHz at a bias voltage of 60 μV. The reasons for saturation of the SQA are discussed.**

***Index Terms*—Josephson devices, RF amplifiers, superconducting devices, superconducting quantum interference devices.**

I. Introduction

THE SQA appears to be a good choice as an IF amplifier integrated with a SIS mixer pumped by a flux-flow oscillator (FFO) in an all-superconducting sub-mm receiver [1], which can be used, for example, for radio astronomy. A semiconductor-based IF amplifier 'integrated' into a fixture of a SIS mixer has demonstrated quite encouraging results [2]. However, use of such amplifiers creates serious problem of heating (10 mW per stage for GaAs HEMT transistors and 1–2 mW—for InP). The SQA has a number of advantages compared to traditional semiconductor amplifiers: ultra-low power consumption, small size and natural compatibility with SIS-based structures. The development of the SQA is a logical step toward integration of superconducting rf devices, that can simultaneously minimize noise, heat and packaging problems in rf detectors. The following applications can be suggested for SQA: i) IF amplifiers for a sub-mm spectrometer based on a Superconducting Integrated Receiver (SIR) with phase-locked loop [3], including SIS Imaging Array receiver [4], ii) quantum limited amplifier for nuclear detectors [5], iii) an amplifier for satellite communication. We have presented in papers [6]–[8] the experimental data on rf SQUID amplifiers that demonstrate feasibility of SQA technology. The present paper contains a detailed analysis of dynamic characteristics of experimental SQA's. Performance limits are discussed.

Manuscript received August 4, 2002. This work was supported in part by the Russian SSP "Superconductivity," RFBR Project 00-02-16270, the INTAS Project 01-0367, the ISTC Project #2445, the Hartmann Foundation, and the Danish Natural Science Council.

G. V. Prokopenko, S. V. Shitov, I. L. Lapitskaya, and V. P. Koshelets are with the Institute of Radio Engineering and Electronics, Russian Academy of Sciences, 101999, Moscow, Russia (e-mail: georgy@hitech.cplire.ru).

J. Mygind is with the Department of Physics, Technical University of Denmark, DK-2800 Lyngby, Denmark (e-mail: myg@fysik.dtu.dk).

Digital Object Identifier 10.1109/TASC.2003.814146

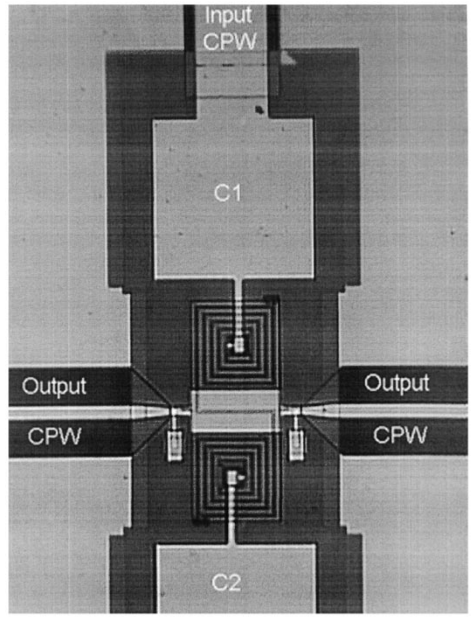

Fig. 1. Photo of central part of SQA chip.

II. SQA RF Design

The basics of microwave design of the S-band SQA with resonant input circuit is described elsewhere [1], [6], [7]. The single-stage SQA consists of a double-washer gradientometer type SQUID, which is formed of two square holes in the ground plane, each of the same size of 60 μm, as shown in Fig. 1. The input coil consists of two identical sections connected in series and positioned inside the corresponding holes of the 'washer'. This configuration yields a small SQUID inductance of about $L_{\mathrm{SQA}} = 70$ pH as well as a sufficiently large coupling coefficient $k^2 \approx 0.6$. The junctions of the SQUID are two $\sim$1 μm^2 Nb-AlO$_X$-Nb resistively shunted SIS junctions. The capacitors $C1$ and $C2$ in the input circuit tune the SQA to the center frequency $f_S \approx 4$ GHz. Two types of SQA's (with balanced and nonbalanced output low-pass filters) are studied. These two types of output circuits correspond to symmetrical and nonsymmetrical biasing of the dc SQUID and provide different magnetic feed-back and thus different flux-voltage characteristics of the device.

The balanced SQA contains two output low-pass filters connected symmetrically to the SQUID as shown in Fig. 1 (left and right connections). These filters have a cut-off frequency of

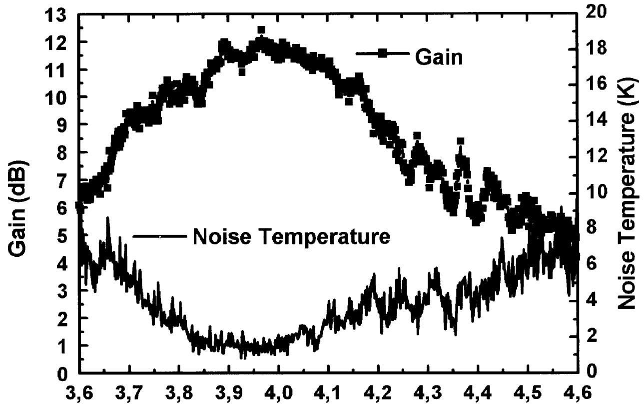

(a)

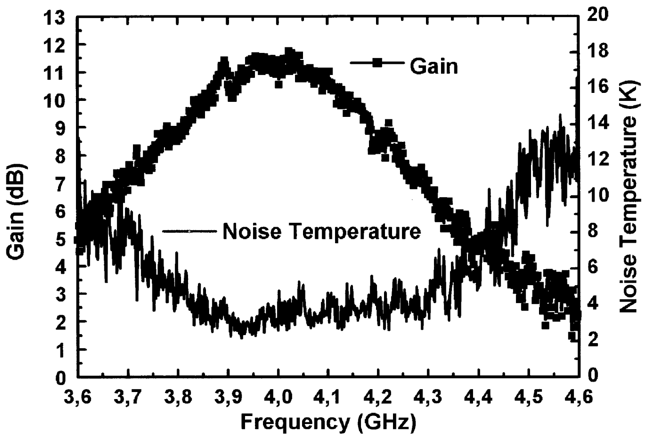

(b)

Fig. 2. (a) Noise temperature and power gain of SQA with $V_c \approx 420\ \mu$V. (b) Noise temperature and power gain SQA with $V_c \approx 345\ \mu$V—for the input signal $T_{\rm IN} \approx 12.5$ K and 30 μV dc voltage bias. The error bars are 1.0 dB and ± 0.5 K, respectively.

TABLE I
MAIN PARAMETERS OF EXPERIMENTAL SQAS.

Type Parameters	Bal .#1	Bal. #2	Non-bal. #1 Positive Feedback	Non-bal. #1 Negative Feedback	Non-bal. #2 Positive Feedback
V_C (μV)	345	420	420	420	290
Gain (dB)	12	11.5	15	6.5	13
Bandwidth 3dB (MHz)	400	500	200	500	200
Min T_N (K)	2.5	1.0	0.5	20	2.5
T_{SAT} (K·GHz)	55	55	22.5	≈250	35

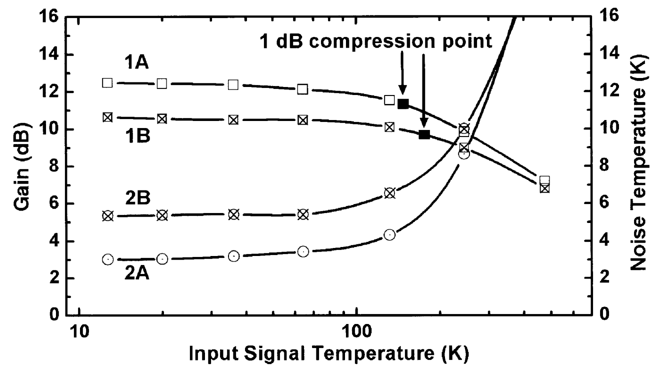

Fig. 3. 1A □ gain, 2A ○ Noise temperature as a function of the input signal for the SQA with $V_c = 420\ \mu$V; 2B ⊠ gain, 2B ⊗ Noise temperature as a function of input signal for the SQA with $V_c = 345\ \mu$V—at the central frequency 4 GHz and 60 μV dc voltage bias.

about 50 GHz that allow for symmetrical bias of the dc SQUID and for transmitting dc bias current and the signal frequency f_S, but preventing the oscillating Josephson current at frequency $f_J \gg f_S$ from leaking out of the SQUID. To adjust the magnetic bias, the common part of the two-loop washer of the SQUID is used as an integrated control line (the light rectangle in the center of Fig. 1. The balanced configuration of the output circuit provides very low direct coupling between input and output circuits of the SQA. The nonbalanced configuration of SQA contains only one output filter, i.e., only one connection shown in Fig. 1 is used for both signal and bias.

III. MEASUREMENTS, RESULTS AND DISCCUSSIONS

To test the amplifiers, the standard hot/cold technique was used. The experimental setup is described elsewhere [3].

A. Balanced Type SQA

A few SQA's with characteristic voltages $V_C \approx 420\ \mu$V [9] ($I_C = 24.5\ \mu$A, $R_N = 17\ \Omega$, we call them 'higher V_C'), and $V_C \approx 345\ \mu$V ($I_C = 16\ \mu$A, $R_N = 21.5\ \Omega$, we call them 'lower V_C'), were tested for noise temperature and gain using a wideband noise signal $T_{\rm IN} \approx 12.5$ K (see Fig. 2 and Table I). The bias point was set at 30 μV, which is about the minimum noise temperature regime. The 3-dB bandwidth, $\Delta f/3$ dB, was found as ≈500 MHz for higher and ≈400 MHz for lower V_C, that correspond to the gain of 12 dB and 11.5 dB respectively. The noise temperature was found (1.0 ± 0.5) K for the SQA with higher V_C and (2.5 ± 0.5) K for the lower one that means inverse proportion to V_C [10]. This tendency is confirmed by our previous measurements [8] performed on samples of the same design, but with much lower $V_C = 100\ \mu$V, where we obtained the following parameters: gain (11 ± 1) dB, 3 dB bandwidth of 300 MHz and noise temperature (4 ± 1) K.

The recent data on SQA gain and noise temperature are presented in Fig. 3 as a function of the input signal temperature $T_{\rm IN}$. The 1 dB compression point corresponds to an input signal of about 120 K for the 500 MHz bandwidth (curve 1 A from Fig. 3) and about 160 K for the 400 MHz bandwidth. The input noise power $P_{\rm IN}$ can be defined as $P_{\rm IN} = k_B \cdot T_{\rm IN} \cdot \Delta f$ where k_B is Boltzmann's constant. The experimental 1-dB gain compression point, $P_{\rm SAT}$, was found to be approximately 1 pW. The saturation temperature within 1 GHz bandwidth, $T_{\rm SAT}^{\rm 1GHz} = P_{\rm SAT}/k_B$, seems to be a convenient measure, since it makes possible estimation for the maximum (saturating) intensity of the source, if its spectrum width is known. The experimental data give $T_{\rm SAT}^{\rm 1GHz} \approx (60 \pm 5)$ K·GHz for a bias voltage of about 60 μV.

The graphs of the SQA gain, noise temperature and the normalized saturation temperature versus bias voltage are shown in Fig. 4. One can see from Fig. 4(a) that the bias voltage of the maximum gain, which is about 40–50 μV, is not the same as that of minimum noise temperature. The saturation temperature increases almost linearly with bias voltage up to 40 μV. Some

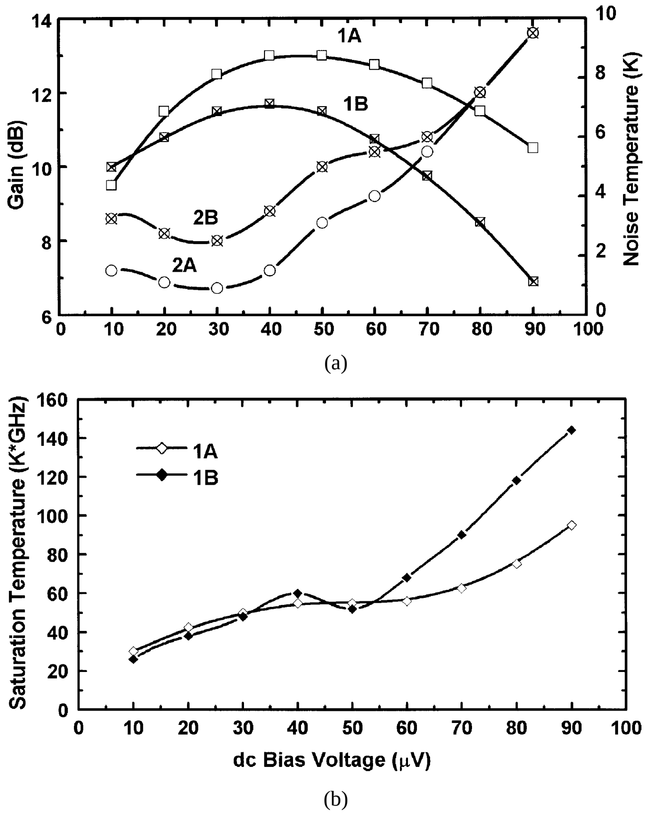

Fig. 4. (a) SQA gain noise temperature: 1A □ gain, 2A ○ Noise temperature as a function of dc bias voltage for SQA with $V_c \approx 420\ \mu$V; 2B ⊠ gain, 2B ⊗ Noise temperature as a function of dc bias voltage for SQA with $V_c \approx 345\ \mu$V; and (b) Saturation temperature for: 1A $V_c \approx 420\ \mu$V, 1B $V_c \approx 345\ \mu$V. All—at the central frequency 4 GHz.

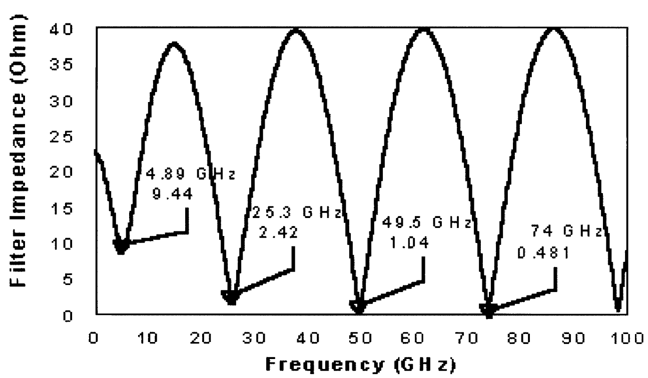

Fig. 5. Modulus of the impedance of output balanced filter.

peculiarity occurs at 50 μV as seen from both graphs (for gain and for noise temperature). This can be explained by parasitic resonances in the output filter. The resonance effect is numerically simulated and presented in Fig. 5 as the modulus of the impedance of the filter at the Josephson junctions of the SQUID. We note here that only third (49.5 GHz) and fourth (74 GHz) resonances are clearly visible in the IV-characteristics of our experimental SQA's. The qualitative explanation can be as following. The resonances produce current steps, which limit the voltage span at the output of the SQA thus affecting both the signal response and saturation power. For this reason the best operation point was found exactly between first and second minima of the modulus at about 30 μV.

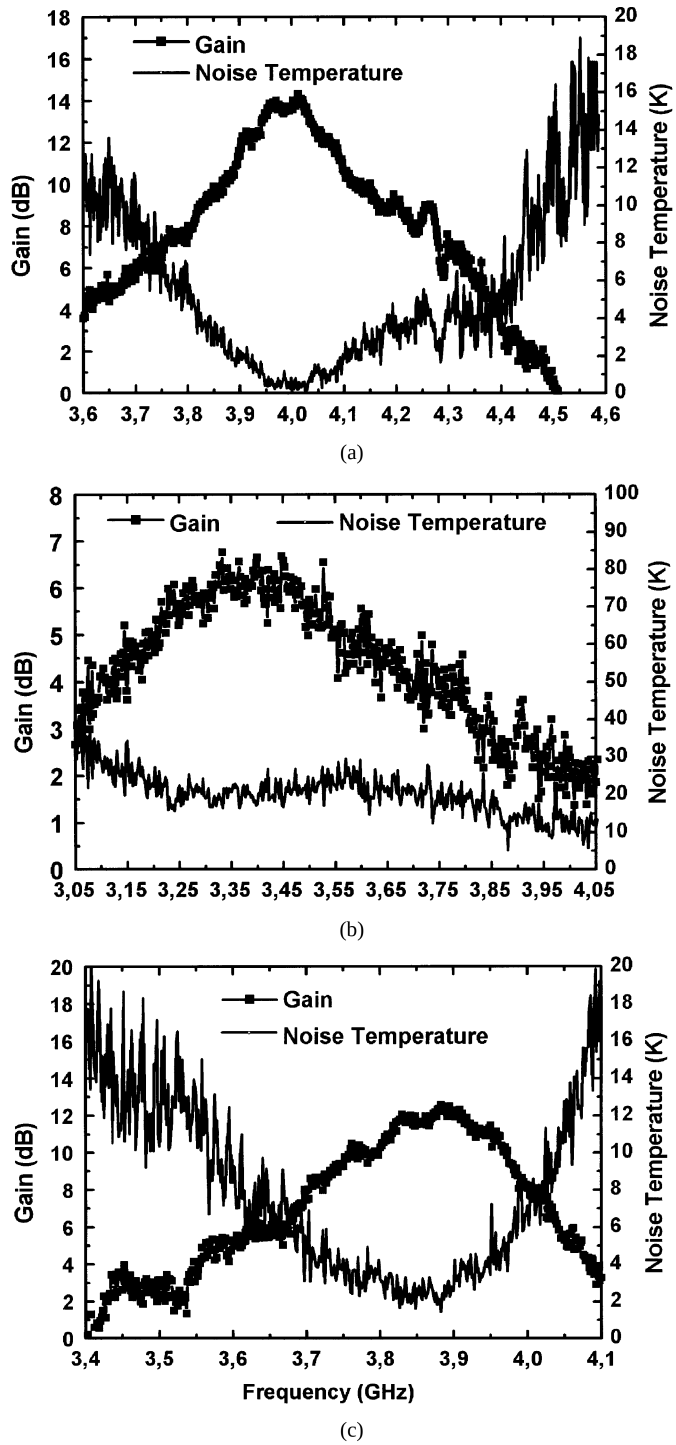

Fig. 6. (a) Noise temperature and power gain of SQA with $V_c \approx 425\ \mu$V; (b) Reverse flux bias for the same SQA; (c) Noise temperature and power gain of SQA with $V_c \approx 290\ \mu$V. All cases are measured with an input signal $T_{\mathrm{IN}}^{\mathrm{HOT}} \approx 12.5$ K at 30 μV dc voltage bias. The error bars are 1.0 dB and $(+0.5/-0.25)$ K, respectively.

B. Unbalanced Type SQA

The unbalanced SQA is provided with asymmetric output connection, as it was mentioned above, that makes the self-field effect appeared at both dc and rf currents. We have experimentally checked this type of amplifier for a feedback effect, which was predicted for this configuration. One can guess that such feedback effect in SQA may change its polarity, dependent on

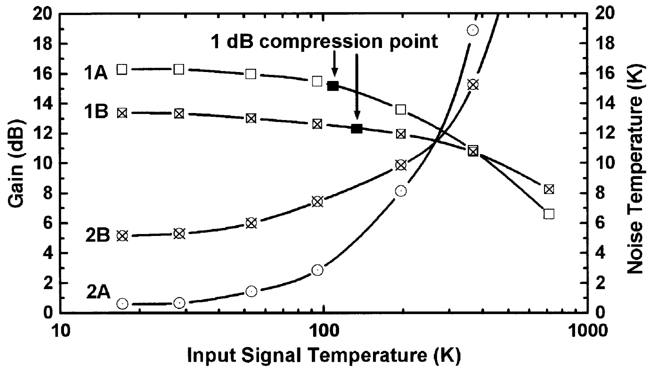

Fig. 7. 1A □ gain, 2A ○ Noise temperature as a function of the input signal for SQA with $V_c \approx 420\ \mu$V; 2B ⊠ gain, 2B ⊗ Noise temperature as a function of input signal for SQA with $V_c \approx 290\ \mu$V: at the central frequency 4 GHz and 60 μV dc voltage bias.

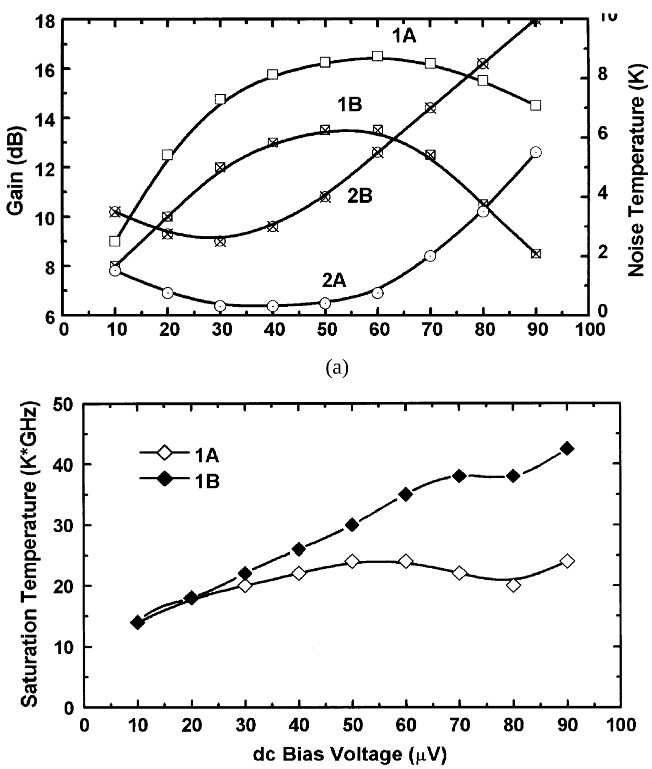

(a)

(b)

Fig. 8. (a) SQA gain and noise temperature: 1A □ gain, 2A ○ Noise temperature as a function of dc bias voltage for an SQA with $V_c \approx 420\ \mu$V; 2B ⊠ gain, 2B ⊗ noise temperature as a function of dc bias voltage for an SQA with $V_c \approx 290\ \mu$V; and (b) Saturation temperature: 1A $V_c \approx 420\ \mu$V, 1B $V_c \approx 290\ \mu$V. All—at the central frequency 4 GHz.

either positive or negative slope of the flux-voltage characteristic is used.

The experimental data presented in Fig. 6 support the theoretical prediction. The gain is found to be larger and the noise temperature is lower for the 'positive' feedback.

The frequency shift of the maximum gain can be attributed to the change of the input impedance of a feedback amplifier. This effect supports our guess that the input impedance of the SQA is far from optimum one and that the best signal coupling from a 50 Ω source takes place at the slope of the resonant curve of the input circuit thus depending on its Q-factor. Figs. 7 and 8 show the main characteristics of the unbalanced SQA. The gain-bandwidth product $G \cdot B \propto V_C$ (where G is the gain, B is the 3-dB bandwidth of rf amplifier) remains approximately the same for experimental samples of different V_C.

IV. Conclusion

The study of the dynamic characteristics of SQA's at 4 GHz has demonstrated that this device can offer a low-noise operation providing $T_N \approx (1\text{–}2)$ K that is about state-of-the-art for coolable HEMT-amplifiers of this frequency range. The saturating signal temperature was found at the level of (100–150) K that, in combination with a bandwidth of about 500 MHz, makes SQA a promising intermediate frequency amplifier, which can be integrated with a SIS mixer or similar superconducting device, e.g., within the fully Superconducting Integrated Receiver.

Acknowledgment

The authors would like to thank O. Pylypenko for fabrication of coolable semiconductor HEMT pre-amplifiers.

References

[1] V. P. Koshelets and S. V. Shitov, "Integrated superconducting receivers," *Supercond. Sci. Technol.*, vol. 13, pp. 53–69, 2000.

[2] S. Padin, D. P. Woody, J. A. Stern, H. G. LeDuc, R. Blundel, C. Y. E. Tong, and M. W. Pospiezalski, "An integrated SIS mixer and HEMT IF amplifier," *IEEE Trans. Microwave Theory Tech.*, vol. 44, pp. 987–990, June 1996.

[3] S. V. Shitov, V. P. Koshelets, L. V. Filippenko, P. N. Dmitriev, V. L. Vaks, A. M. Baryshev, W. Luinge, N. D. Whyborn, and J.-R. Gao, "A superconducting integrated receiver with phase-lock loop," in *Inst. Phys. Conf. Ser. no. 167*, 2000, pp. 647–650.

[4] S. V. Shitov, V. P. Koshelets, A. B. Ermakov, L. V. Filippenko, A. M. Baryshev, W. Luinge, and J. R. Gao, "Superconducting chip receivers for imaging application," *IEEE Trans. on Appl. Supercond.*, vol. 9, pp. 3773–3776, June 1999.

[5] M.-O. André, M. Mück, J. Clarke, J. Gail, and C. Heiden, "Radio-frequency amplifier with tenth-kelvin noise temperature based on a microstrip direct current superconducting quantum interference device," *Appl. Phys. Let.*, vol. 75, pp. 698–700, Aug. 1999.

[6] G. V. Prokopenko, S. V. Shitov, V. P. Koshelets, D. V. Balashov, and J. Mygind, "A DC SQUID based low noise 4 GHz amplifier," *IEEE Trans. Appl. Supercond.*, vol. 7, pp. 3496–3499, June 1997.

[7] G. V. Prokopenko, D. V. Balashov, S. V. Shitov, V. P. Koshelets, and J. Mygind, "Two-stage S-band DC SQUID amplifier," *IEEE Trans. Appl. Supercond.*, vol. 9, pp. 2902–2905, June 1999.

[8] G. V. Prokopenko, S. V. Shitov, D. V. Balashov, P. N. Dmitriev, V. P. Koshelets, and J. Mygind, "Low-noise S-band DC SQUID amplifier," *IEEE Trans. on Appl. Supercond.*, vol. 11, pp. 1239–1242, Mar. 2001.

[9] P. N. Dmitriev, I. L. Lapitskaya, L. V. Filippenko, A. B. Ermakov, S. V. Shitov, G. V. Prokopenko, S. A. Kovtonyuk, and V. P. Koshlets, High Quality Nb-Based Integrated Circuits for High Frequency and Digital Applications. in this volume.

[10] K. K. Likharev, *Dynamics of Josephson Junctions and Circuits*: Gordon and Breach Science Publishers, 1986.